

UCLA

UCLA Previously Published Works

Title

Signatures of adaptive evolution in platyrrhine primate genomes.

Permalink

<https://escholarship.org/uc/item/37f9r10q>

Journal

Proceedings of the National Academy of Sciences of the United States of America,
119(35)

Authors

Byrne, Hazel

Webster, Timothy

Brosnan, Sarah

et al.

Publication Date

2022-08-30

DOI

10.1073/pnas.2116681119

Peer reviewed



Signatures of adaptive evolution in platyrrhine primate genomes

Hazel Byrne^{a,b,1} , Timothy H. Webster^a , Sarah F. Brosnan^c , Patrícia Izar^{d,2}, and Jessica W. Lynch^{b,e,2}

Edited by Scott Edwards, Harvard University, Cambridge, MA; received September 9, 2021; accepted July 7, 2022

The platyrrhine family Cebidae (capuchin and squirrel monkeys) exhibit among the largest primate encephalization quotients. Each cebid lineage is also characterized by notable lineage-specific traits, with capuchins showing striking similarities to Hominiidae such as high sensorimotor intelligence with tool use, advanced cognitive abilities, and behavioral flexibility. Here, we take a comparative genomics approach, performing genome-wide tests for positive selection across five cebid branches, to gain insight into major periods of cebid adaptive evolution. We uncover candidate targets of selection across cebid evolutionary history that may underlie the emergence of lineage-specific traits. Our analyses highlight shifting and sustained selective pressures on genes related to brain development, longevity, reproduction, and morphology, including evidence for cumulative and diversifying neurobiological adaptations across cebid evolution. In addition to generating a high-quality reference genome assembly for robust capuchins, our results lend to a better understanding of the adaptive diversification of this distinctive primate clade.

capuchin monkeys | positive selection | comparative genomics | brain evolution | Cebidae

Platyrrhine primates (also known as neotropical primates) present an interesting example of the adaptive diversification of a primate clade into diverse ecological niches. Platyrrhines of South and Central America and catarrhines of Africa and Asia (and extinct forms from Europe) likely diverged via transatlantic dispersal of the platyrrhine ancestor from Africa to South America (1–3) 40 to 44 Ma (4, 5), with the earliest South American fossils at ~36 Ma resembling small Eocene African anthropoids (6), and a more extensive South American primate fossil record starting at 26 Ma (7–11). Primate diversification within South America has included Patagonian taxa and Greater Antillean taxa, both now extinct and hypothesized to be a stem group and the sister group to modern platyrrhines, respectively (10), although others argue some of these fossils belong within several clades of extant platyrrhines (12–14). The crown platyrrhine radiation began to diversify 19 to 26 Ma (4, 5, 10, 15, 16), with most of the extant diversity contained in the rainforests of Amazonia and the Atlantic Forest biome (17). Based on fossil evidence, paleogeology, and statistical biogeographic analyses, it has been suggested that ecological opportunity across multidimensional niches in expanding rainforest environments may have driven the diversification of major platyrrhine lineages (18, 19), leading to the evolution of over 20 extant genera and 170 extant species (20, 21). Platyrrhine primates show striking phenotypic diversity in body and brain size, skeletal morphology, pelage patterns, group size, social and mating systems, life history and longevity, behavioral plasticity, and diet and dietary adaptations, among many other traits, with this diversity becoming increasingly well-characterized in recent years. We know very little, however, about the genetic changes involved in the evolution of this array of diversity and where in the platyrrhine clade those changes occurred.

Extant platyrrhine diversity is accommodated within five families which diversified by the late Miocene: Atelidae (spider monkeys and howler monkeys), Pitheciidae (sakis and titi monkeys), Aotidae (owl monkeys), Callitrichidae (marmosets and tamarins), and Cebidae (squirrel monkeys and capuchins) (10, 20, 22; reviewed in ref. 23). Cebids form a clade with callitrichids and aotids, to the exclusion of pitheciids and atelids, though the position of aotids in relation to cebids and callitrichids is poorly resolved as these three taxa diversified rapidly in the late Miocene (16, 24). Within the family Cebidae, genus-level relationships among extant taxa are clearly defined, with squirrel monkeys (*Saimiriinae*) as the sister group to capuchins (*Cebinae*). Utilizing both fossil and morphological evidence, squirrel monkeys and capuchins are estimated to have diverged by at least 14 Ma (4, 5, 25). The late Miocene fossils, *Neosaimiri fieldsi* and *Laventiana annectens*, display many derived squirrel monkey characteristics (8, 22, 26–29).

While all major platyrrhine groups show lineage-specific traits, the family Cebidae (capuchin and squirrel monkeys) is compelling considering its members' large encephalization

Significance

Primates of South and Central America known as platyrrhines show broad phenotypic diversity, but we know very little about the genetic changes underlying this diversity or at what point during platyrrhine evolutionary history they arose. Particularly notable are capuchin monkeys for their many parallels with humans and apes, including large brains, intelligence, long lives, and tool usage. Here, we generate a set of high-quality, manually curated protein-coding alignments for comparative genomic analysis of platyrrhines, focusing on the family Cebidae (capuchin and squirrel monkeys). We uncover signatures of selection related to brain development and other cebid traits, lending insight into major periods of cebid adaptive evolution and the evolutionary mechanisms underlying convergence between capuchins and apes.

Author contributions: H.B., P.I., and J.W.L. designed research; H.B. and J.W.L. performed research; S.F.B. contributed new reagents/analytic tools; H.B. analyzed data; H.B., T.H.W., P.I., and J.W.L. wrote the paper; T.H.W. provided data interpretation and supervision; S.F.B. provided sampling contributions and helped with writing; and P.I. provided data interpretation.

The authors declare no competing interest.

This article is a PNAS Direct Submission.

Copyright © 2022 the Author(s). Published by PNAS. This article is distributed under [Creative Commons Attribution-NonCommercial-NoDerivatives License 4.0 \(CC BY-NC-ND\)](https://creativecommons.org/licenses/by-nc-nd/4.0/).

See [online](#) for related content such as Commentaries.

¹To whom correspondence may be addressed. Email: byrne.hazel1@gmail.com.

²P.I. and J.W.L. contributed equally to this work.

This article contains supporting information online at <http://www.pnas.org/lookup/suppl/doi:10.1073/pnas.2116681119/-DCSupplemental>.

Published August 22, 2022.

quotient (relative brain to body size), with reconstructions showing one of the fastest increases in encephalization quotient across primates along the ancestral Cebidae branch (30). Together, cebids are unique among platyrrhines in that they retain a generalized arboreal quadruped body plan; are extremely rapid and alert and have high energy budgets; consume more insects than expected given body size; and form large, gregarious groups, usually with female philopatry, multimale multifemale social organization, and polygynandrous mating patterns, quite unlike the pair-bonded or polyandrous social organization and mating patterns seen in their sister taxa (Callitrichidae and Aotidae) (20, 31). Cebinae are more than three times the size of *Saimiri* and they show striking differences in head size and shape, but both have large brain-to-body-size ratios compared to other platyrrhine taxa. Rosenberger (32) classified Cebidae as frugivore-insectivores but noted that *Saimiri* have more insectivorous specializations, such as puncture-crushing teeth and highly convergent orbits, whereas capuchins are more generalized omnivores. Developmental studies have shown that key cranial morphological differences between Saimiriinae and Cebinae are attributable mostly to scale or absolute size; the two subfamilies follow the same allometric trend and differences are possibly related to a heterochrony in development due to delayed growth and reproduction in capuchins (33). Marroig (33) classifies Cebidae together as paedomorphic compared to other platyrrhines but squirrel monkeys as paedomorphic compared to capuchins.

The subfamily Cebinae (capuchins) are a particularly remarkable contrast to other platyrrhines for their many striking similarities to Hominidae, including social conventions and traditions, complex relationships, high dexterity, sensorimotor intelligence with tool use and extractive foraging, advanced derived cognitive abilities, diverse behavioral repertoire and flexibility, and slow maturation (31). These traits are uncommon or absent among other platyrrhines and it is of great anthropological interest to gain insight into the evolutionary mechanisms underlying the independent emergence of these convergent traits and their associated genomic changes. The existence of two capuchin genera (*Cebus* and *Sapajus*) which diverged within a timeframe similar to *Homo* and *Pan* brings further interest to understanding their distinct evolutionary histories. Although in many respects *Cebus* and *Sapajus* are similar, major differences exist in morphology, ecology, and behavior (see ref. 34 for review). Behaviorally, both learn socially; however, *Sapajus* shows greater tool use, including nut cracking similar to that seen in apes, whereas *Cebus* shows more group-level social traditions (35, 36). These behavioral differences have been linked to both cognitive evolution and ecological factors; *Sapajus* may have adapted to resource scarcity through tool use whereas *Cebus* relied on coalitionary support. *Cebus* is more of a ripe fruit specialist, whereas *Sapajus* has robust cranial and postcranial skeletal and dental morphological adaptations affording greater access to hard-object foods (37–40). The capuchin genera diverged by 5 to 6 Ma based on fossil-calibrated molecular phylogenies (41–43), while fossils such as *Acrecebus* (44, 45) (estimated at over 15 kg) show a robust capuchin morphology had emerged by 6 to 9 Ma.

The genus *Saimiri* (squirrel monkeys, subfamily Saimiriinae), the sister group to Cebinae, are also characterized by slow maturation and large encephalization quotient, with a larger working memory span than marmosets, a neocortex-to-brain ratio far exceeding that of marmosets, and evidence for age-related cognitive decline paralleling humans (reviewed in ref. 46). *Saimiri* are hypergregarious, with the largest stable social groups among platyrrhines, and frequently engage in mixed-species

associations, especially with capuchins (47). They are also a key primate biomedical model with foci on neuroendocrinology, ophthalmology, pharmacology, behavior, viral persistence, infectious diseases, cancer treatment, and reproductive physiology, among others (48).

Here, we take a comparative genomics approach to uncover signatures of adaptive evolution in cebid genomes to better understand the adaptive diversification of this distinctive platyrrhine primate clade. We focus on the three extant cebid lineages—robust capuchins (genus *Sapajus*), gracile capuchins (genus *Cebus*), and squirrel monkeys (genus *Saimiri*)—as well as the ancestral capuchin (Cebinae) and ancestral Cebidae branches. Our study highlights the evolutionary history of Cebidae since their divergence from other platyrrhines, focusing on derived characteristics shared among cebid lineages, shared across capuchins that emerged after their divergence from squirrel monkeys, and unique to each of these three extant cebid genera. Through the analysis of successive lineages in the cebid clade, we are able to gain insight into major periods of cebid adaptive evolution in a branchwise manner and identify candidate adaptive genes that may underlie the emergence of lineage-specific traits. Previous work assessing signatures of adaptive evolution in protein-coding regions for cebid lineages considered the entire capuchin subfamily (Cebinae) together as represented by a single species (*Cebus imitator*), uncovering broad signatures of positive selection on the brain and DNA repair (which was associated with longevity) (49), or focused on signatures of convergence among encephalized primate lineages including humans (50). This work greatly expands upon these existing studies by individually analyzing five distinct cebid branches, separately analyzing three lineages of Cebinae (*Sapajus*, *Cebus*, and ancestral Cebinae) as well as two further lineages, ancestral Cebidae and squirrel monkeys (*Saimiri*), to infer the targets of selection during various periods of cebid evolution.

Results

Robust Capuchin Reference Genome. At the start of this study, annotated genome assemblies were publicly available for *Cebus imitator* and *Saimiri boliviensis*. We generated a genome assembly for *Sapajus apella* using short-read data (~148-fold coverage) scaffolded with Dovetail's Chicago proximity ligation libraries (*SI Appendix, Table S1*) using their HiRise pipeline (51). Total length of this genome assembly was 2,520 Mbp (in 6,631 scaffolds) with an N50 of 27.1 Mbp (29 scaffolds) and N90 of 4.04 Mbp (116 scaffolds). We identified 91.5% (5,666) of BUSCO's (52) Euarchontoglires-specific conserved single-copy orthologs in the assembly including 85% (5,264) complete (with 0.6% duplicated) and 6.5% (402) fragmented, and 90.3% (224) of CEGMA's (53) core eukaryotic genes (CEGs). Together, assembly metrics and genome completeness based on gene content indicate a contiguous, high-quality reference genome assembly for robust capuchins (*Sapajus*). We estimated genome size with filtered short-read data based on *k*-mer (31-mer) frequencies using the four approaches, resulting in an estimated haploid genome length for our *S. apella* reference individual between 2,918 and 3,029 Mbp (*SI Appendix, Table S2*). Previous estimates of genome size for other robust capuchin species, *Sapajus libidinosus* and *Sapajus nigritus*, estimated using Feulgen image analysis densitometry, ranged between 3,276 and 3,374 Mbp and 2,921 and 3,025 Mbp, respectively (54). These estimates, in particular for *S. nigritus*, are very similar to our estimates for *S. apella* calculated in this study.

We pooled raw RNA-sequencing (RNAseq) data (367 million read pairs) derived from total RNA from 17 tissues from the same reference individual and, postfiltering, retained 341 million read pairs (*SI Appendix, Table S3*). We assessed quality metrics and completeness of the seven transcript assemblies generated using cleaned RNAseq read pairs with rnaQUAST (55) and BUSCO, which revealed that upward of 94% of the transcripts aligned to the genome with an average aligned percentage of greater than 92.7%, and indicated the final assemblies used in downstream analyses (TrinDNv2, PASAv1, and NRv1) were high-quality, near-complete transcriptomes (~96 to 97% complete) (*SI Appendix, Table S4*). Repeat annotation of the genome assembly using libraries of both known and de novo elements estimated the total interspersed content of the genome as 43.02% (1.06 Gbp) and total annotated repeat content (including transposable elements as well as small RNA, satellites, simple repeats, and low complexity repeats) as 44.63% (1.12 Gbp) (*SI Appendix, Table S5*). After three iterations of Maker (56, 57) to predict and annotate gene models in the robust capuchin genome assembly (*SI Appendix, Table S6*) and subsequent filtering, we recovered 25,279 predicted genes for *S. apella* for downstream analyses.

Ortholog Alignment and Branch/Branch-Site Model Tests. We initially identified 12,160 one-to-one orthologs recovered in at least 2 of the 10 species we used in our comparative genomic analyses; these include nine primates, of which four are platyrrhines, and mouse (Fig. 1 and *SI Appendix, Table S7*). After filtering for a minimum of five species and the presence of at least one capuchin lineage (gracile or robust), alignment using Guidance2 (58) with 100 bootstraps, and filtering for errors to reduce the likelihood of false positives, we retained a set of 9,216 conservative, manually curated coding sequence (CDS) alignments which were highly likely to represent one-to-one ortholog groups across their length. Detailed information on each of the final alignments, including group ID, assigned gene symbol, and Entrez ID, can be found in *SI Appendix, Table S8*. In total, there were 207 different combinations of species (species sets) represented in the final alignments (*SI Appendix, Table S9*), with most alignments assigned to the set of all species (full) ($n = 4,636$) or sets with nine species ($n = 2,819$) and the rest to sets with between eight and five species ($n = 1,761$) (Table 1 and *SI Appendix, Table S10*).

These 9,216 alignments were used as input to our codon-based models of evolution based on nonsynonymous versus

synonymous substitutions (ω or dN/dS ratio) to identify candidate genes under selection in six cebid lineages of interest (Fig. 1): H1, robust capuchin (*Sapajus*); H2, gracile capuchin (*Cebus*); H3, ancestral Cebinae (capuchins); H3a, across-capuchins (all Cebinae; branches H1, H2, and H3 combined); H4, ancestral Cebidae (i.e., ancestor to capuchins and squirrel monkeys); and H5, squirrel monkey (*Saimiri*). In total we tested 11 lineage and test combinations using codeml from PAML (59), branch models (BM) across all six lineages, which tests for elevated dN/dS ratios along the target branch indicating accelerated evolution, and branch-site models (BSM) across five lineages (excluding H3a), which tests for episodic selection by searching for positively selected sites in the target lineage. Groups (alignments) analyzed per lineage varied between 6,978 and 9,003 of 9,216 total (Table 1 and *SI Appendix, Table S10*), with averages of 7,957 BM and 7,748 BSM tests.

Across the six lineages analyzed for BM, we recovered 248 to 552 (average 351) models with signatures of accelerated evolution ($P < 0.05$ before correction for multiple testing). In contrast, across the five lineages analyzed for BSM, we found 75 to 186 (average 113) models with signatures of episodic positive selection ($P < 0.05$ before correction for multiple testing), much fewer than for BM tests particularly for shorter branches for the capuchin lineages. Between 17 and 34 (average 25) groups have signatures for both BM and BSM tests for the same lineage (Table 1 and *SI Appendix, Table S10*). Lists of all groups (genes) analyzed for each of the six lineages can be found in *SI Appendix, Tables S11–S16*. More detailed information for the groups with putative evidence of accelerated evolution or episodic selection from the BM and/or BSM tests (groups that were significant precorrection for multiple testing) including P values, likelihood ratio test (LRT) statistics, and likelihood scores is given in *SI Appendix, Tables S17–S22*.

After correction for multiple testing procedures, there were no or very few (five or fewer) significant genes for all BSM tests and most lineages for BM tests. This small number of genes retained after correction for multiple testing is in strong contrast to comparable studies on nonhuman primates. We consider this discrepancy a result of our strict manual curation process which drastically reduces the occurrence of false positives. We therefore consider the significant false discovery rate (FDR)-corrected genes to be very strong candidates for adaptively evolving genes and the overall set of significant genes according to uncorrected P values to be the most likely set of genome-wide candidates from the background set for each

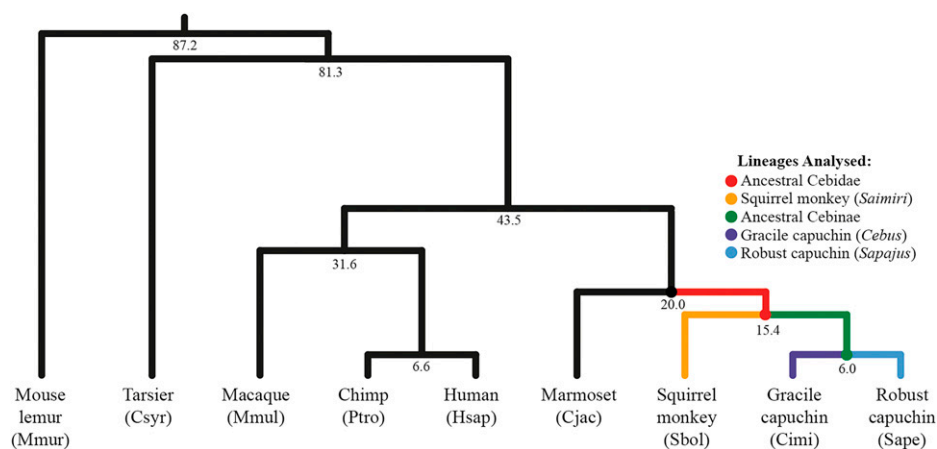


Fig. 1. Reconstructed chronogram showing the primate consensus guide tree topology used in this study and the cebid branches assessed for signatures of positive selection. Divergence date point estimates (in millions of years ago) are from ref. 4.

Table 1. Counts of groups and candidate adaptively evolving genes for BM and BSM tests with PAML

	Total groups	Groups with all species	Groups with 9 species	Groups with <9 species	Candidate models: BM	Candidate models: BSM	Overlap BM & BSM
Robust capuchin (H1)	7,010	4,636	1,695	679	292	80	17
Gracile capuchin (H2)	7,010	4,636	1,695	679	248	75	18
Ancestral Cebinae (H3)	6,978	4,636	1,695	647	302	122	30
Across-Cebinae (H3a)	9,003	4,636	2,756	1,611	552	NA	NA
Ancestral Cebidae (H4)	8,740	4,636	2,701	1,403	278	104	26
Squirrel monkey (H5)	9,003	4,636	2,756	1,611	435	186	34
Average	7,957	4,636	2,216	1,105	351	113	25

NA, not applicable.

lineage. We refer to these sets of genes as candidate adaptively evolving genes and our gene set enrichment analyses are conducted on the set of candidate adaptively evolving genes for each lineage for each test (11 sets in total). Detailed justification for our distinct approach is provided in *SI Appendix*.

Gene Set Enrichment. Gene set enrichment analyses using DAVID v.6.8 (60) for each set of candidate adaptively evolving genes from each combination of lineage and test (six BM and five BSM) aided interpretation of the biological significance of the results. We assessed lists of enriched BP (biological process), CC (cellular component), and MF (molecular function) Gene Ontology (GO) terms, UP keywords, KEGG pathways, Reactome pathways, and disease annotations, as well as functional annotation clustering across the three GO terms together under the high classification stringency criteria, with an EASE score of <0.05 required for all enriched annotated terms and a minimum enrichment score of 1.3 for all annotation clusters. Across all lineages for the BM and BSM gene sets we recovered between 2 and 13 (average 6) and 0 and 9 (average 3) GO clusters and 68 and 189 (average 103) and 10 and 123 (average 60) enriched terms (all annotation categories), respectively (*SI Appendix, Table S23*). Information on each of the enriched annotated terms and GO clusters including description, gene counts and hits and statistical results such as EASE score and fold enrichment for each gene set enrichment analysis is found in *SI Appendix, Tables S24–S44*. A detailed written summary of the gene set enrichment results for each lineage is presented in *SI Appendix*.

Discussion

Our analyses reveal signatures of positive selection on many lineage-specific traits across Cebidae and highlight branches with putative selective pressure on genes related to brain development and function, longevity, behavior, reproduction, and morphology (Fig. 2). Perhaps most striking are the sustained signatures of positive selection recovered on brain evolution across Cebidae, which appear early in cebid history with subsequent selection on different aspects of central nervous system (CNS) development at various time intervals for different lineages. While we recover an evolutionary history of encephalization beginning in ancestral Cebidae and continuing independently in squirrel monkeys and capuchins, the strongest evidence for selection on neuroplasticity and behavioral flexibility is found for ancestral Cebinae or the entire capuchin clade when considered together (across-capuchins). The most striking signatures of selection recovered independently for the capuchin genera relate to their body shape and skeletal morphology, including the distinctive robust cranial and skeletal morphology in robust capuchins (*Sapajus*), and, conversely, the gracile limb morphology

associated with more rapid, agile movement in gracile capuchins (*Cebus*). All three extant cebid genera are long-lived for their body size, and each shows signatures of selection on genes related to aging, longevity, and/or neurodegeneration. In addition, in contrast to other closely related taxa, all three cebid genera live in relatively large groups with polygyny and complex sexual interactions, and we recover signatures of sustained positive selection related to sperm production/morphology and reproductive behavior. Our comparative approach to uncovering candidate targets of positive selection within Cebidae highlights shifting and sustained selective pressures within this clade, including evidence for cumulative and diversifying neurobiological adaptations over cebid evolutionary history. In the following sections, we discuss our results describing adaptive evolutionary change in these lineages across various biological categories.

Neurodevelopment and Plasticity. A major hallmark of primate evolution is expansion of the brain, with numerous independent shifts to larger brain mass relative to body size also occurring among different primate lineages. Larger brains have long been associated with increased cognitive capabilities, higher social complexity, and increased ability to respond to environmental and socioecological challenges (61). The most encephalized primates after humans are platyrrhines of the family Cebidae—capuchins and squirrel monkeys (49, 50)—and ancestral state reconstructions have indicated that the second-fastest increase in the rate of encephalization across primates occurred along the ancestral Cebidae branch (30). Overall, our results are consistent with an evolutionary history of encephalization and adaptive brain evolution beginning in ancestral Cebidae and continuing independently in both squirrel monkeys and capuchins after their divergence around 13.8 Ma (25).

We recovered signatures of selection and accelerated evolution on the CNS that may be associated with this encephalization shift—in particular, related to brain development and patterning. For the ancestral Cebidae branch, we recovered the enriched CC term “growth cone,” a motile, sensory structure that plays a critical role in precisely specified brain wiring patterns, guiding axons to their targets during neural development, and is also essential in the mature brain for plasticity-dependent synaptogenesis (62). Growth cone dynamics and axonal tract development are regulated by ciliary signaling (63), and, notably, some of the strongest selective signatures for ancestral Cebidae are related to the cilium (both primary and motile, as well as microtubules). Many of the most enriched terms are cilium-specific and including genes with essential roles in ciliogenesis and implicated in the ciliopathy Joubert’s syndrome. Primary cilia are found in almost all mammalian cells and the range of symptoms characterizing ciliopathies highlights the difficulty in associating the signal of selection on cilium with a single adaptive

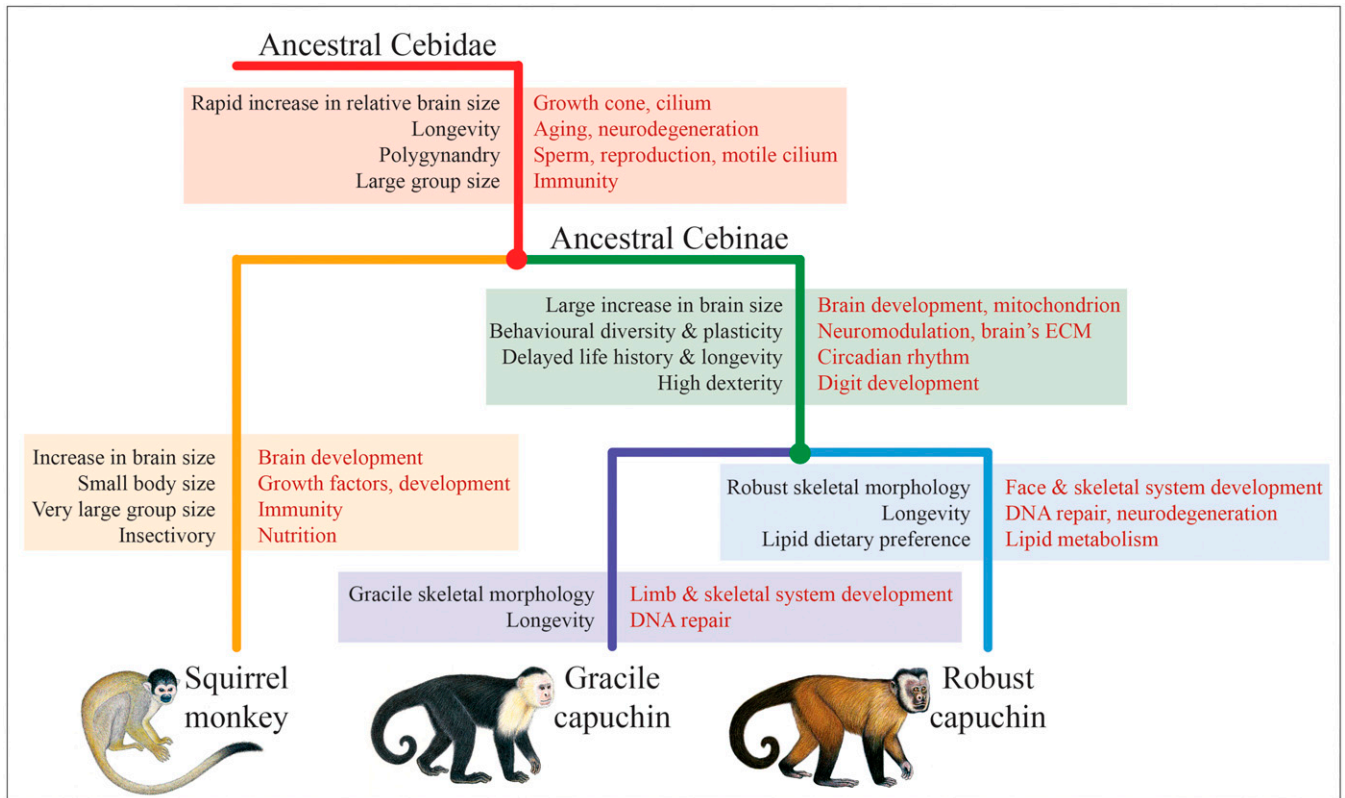


Fig. 2. Graphic summary of select signatures of adaptive evolution per cebid lineage. On the left are traits associated with each branch, which for the ancestral lineages are inferred based on traits shared by all daughter lineages. Brain size changes are based on ref. 30. On the right (in red text) are the associated signatures of adaptive evolution. Illustrations by Stephen Nash.

function; it is notable, however, that many of these disorders are characterized by pronounced neurodevelopmental abnormalities. Primary cilia are critical to the development of the CNS, playing essential roles in early patterning, neurogenesis, and neuronal migration and connectivity, at least in part owing to their essential role in mediating signal transduction in key signaling pathways (64). Taken together, these results suggest adaptive evolution of the CNS and brain patterning in ancestral Cebidae, which may be linked to the increase in brain size found along this branch.

After the Cebinae/Saimiriinae divergence, relative brain size of both squirrel monkeys and capuchins is modeled to have increased independently at a similar rate. For squirrel monkeys, it is explained by a reduction in body size and moderate increase in brain size, while for capuchins it is driven by a large increase in brain size along with a smaller increase in body size (30). In agreement with this, we find continued brain-related signatures of selection in both lineages. For squirrel monkeys, we recovered various enriched brain-related GO terms for the BSM gene set including “regulation of neuron differentiation,” “nervous system development,” and “neurogenesis,” among others. A gene in the squirrel monkey gene set is *ADCYAP1*, which is accelerated in humans and has been associated with human brain-size evolution (65). Some of these signatures for squirrel monkeys may also relate to the adaptive maintenance of a large brain size while reducing body size.

Capuchins are particularly notable for their large brains and high encephalization quotients, the latter second only to humans among primates (66), and other hallmarks of their evolution include their derived cognitive abilities, sensorimotor intelligence, diverse behavioral repertoire, and extensive behavioral plasticity (31). Capuchins show striking convergence with great apes

(particularly humans) across these traits, which are uncommon among other platyrrhines. Related to these traits, we recover the enriched BP GO term “CNS development” (BSM gene set) for ancestral Cebinae with important developmental genes such as *GDF7*, which contributes to neuronal cell identity in the developing embryonic nervous system. As with ancestral Cebidae, we also find signatures of enrichment related to cilia for ancestral Cebinae (in both gene sets) with several genes involved in primary cilium function that are also found in the “CNS development” GO term (such as *CEP162* and *BBS7*) and implicated in ciliopathies including Seckel and Bardet–Biedl syndrome. Orkin et al. (49) also found signatures of adaptive evolution related to brain development and neurogenesis for *C. imitator*. Importantly, however, our study places these positive selection pressures for brain development as most strongly affecting the ancestral Cebidae and Cebinae lineages; this suggests that brain organization and function may have become relatively stable with only minor divergence across the two capuchin genera despite their subsequent divergent ecological and morphological adaptations (but see below for some brain-related genes of interest).

Behavioral repertoires are manifestations of neural activity and changes in behavior are ultimately followed by alterations in neuronal connectivity, i.e., neuroplasticity (67). We found further brain-related signatures for capuchins putatively associated with this trait. Two highly ranked genes in the “CNS development” GO term for ancestral Cebinae encode chondroitin sulfate proteoglycans of the lectican family that are specifically expressed in the CNS: *NCAN* (neurocan), the fourth-ranked gene in the BSM gene set, and *BCAN* (brevican), the second-ranked gene in the BM gene set and also in the BSM gene set. These chondroitin sulfate proteoglycans serve as guidance cues during brain development as well as play important roles in neuroplasticity by

modulating synaptic connections in the adult brain. They are abundant components of the brain's extracellular matrix, forming condensed lattice-like structures known as perineuronal nets that form as one of the ultimate acts coinciding with the closure of critical periods for experience-dependent plasticity. The relationship between neurons and perineuronal nets is a central mechanism controlling neuroplasticity, with perineuronal nets playing many important roles in CNS functions including regulating synaptic plasticity, stabilizing synapses, and neuroprotection. They are involved in cognition through encoding, maintaining, and updating memories, as well as recovery after nervous system damage, psychiatric disease, and neurodegeneration (68, 69). It is therefore significant that two of the most central and abundant components of perineuronal nets, the chondroitin sulfate proteoglycans, brevican (*BCAN*) and neurocan (*NCAN*), show strong signatures of selection in ancestral Cebinae, with *BCAN* also selected in *Cebus* and *NCAN* also selected in *Sapajus*. Indeed, signatures of selection potentially related to synaptic plasticity appeared even earlier along the ancestral Cebidae branch given the importance of the growth cone for plasticity-dependent synaptogenesis, as discussed.

The behavioral diversity characterizing capuchin monkeys includes social conventions and local traditions, complex and intimate social relationships, ecological and dietary flexibility, tool use, and extractive foraging including an astounding degree of planning, with capuchin behavior varying by age, sex, and geographically across populations of the same species (34, 35, 70–72). We recover broad signatures of selection on neuropeptides and hormones for the cebine branches, particularly for ancestral Cebinae and across-capuchins. Interesting genes found across these annotations include those encoding neuropeptides and receptors that play important roles in many physiologic processes such as cognition, memory, sensory/pain processing, stress, hormone and insulin secretion, and appetite regulation. There are also multiple genes in the hormone annotations in the ancestral Cebinae and/or across-capuchin gene sets related to the thyroid hormone and thyroid-stimulating hormone (e.g., *TRH*, *CGA*, and *PAX8*). Thyroid hormone is a key metabolic hormone with many physiologic functions including critical roles in differentiation, growth, and metabolism. It dramatically impacts mammalian brain development, with its importance highlighted by the deleterious and irreversible effects of thyroid hormone deficiency/dysfunction during fetal and neonatal periods. Thyroid hormone also plays important roles in normal adult brain function and has a profound influence on behavior throughout life, with adult-onset thyroid hormone dysfunction associated with a range of CNS-related pathologies, neurological and behavioral abnormalities, and alterations in mood and cognition (73).

For the across-capuchin gene set, we recover signatures related to neurotransmission and vesicle fusion including six genes encoding synaptotagmin and synaptotagmin-like proteins which are known to play important roles in regulated neurotransmitter release and hormone secretion. Among these genes is *SYT11*, which forms an essential component of a neuronal vesicular trafficking pathway crucial for development and synaptic plasticity and plays an important role in dopamine transmission (74). Other related genes for the across-capuchin gene set are involved in the regulation of synaptic AMPA receptors, which play a key role in synaptic plasticity, being involved in long-term potentiation and depression of synaptic transmission in the hippocampus and encoding or interacting with neuroligins, neuronal cell-surface proteins involved in synaptic contacts and transmission.

Although the brain-related signatures are strongest for the ancestral cebid lineages, we also find distinct accelerated genes related to neurodevelopment in each of the capuchin genera, suggesting some, perhaps minor, continuation of adaptive brain evolution independently in robust and gracile capuchins after their divergence around 5 to 6 Ma. This signature is more notable for robust capuchins; we recover enriched terms related to cilia including the UP keywords “cilium” and “Bardet–Biedl syndrome” and the CC GO term “MKS complex,” covering three genes involved in ciliogenesis and required for the formation of primary nonmotile cilium. One of these is *AH11*, which is required for both cerebellar and cortical development in humans and may play a crucial role in ciliary signaling during cerebellum embryonic development as a positive modulator of classical Wnt signaling (75). *AH11* also shows an accelerated rate of evolution along the human lineage since the split from chimpanzees and bonobos (76). For gracile capuchins, the enriched UP keyword “developmental protein” contains multiple genes with important roles in CNS development.

Mitochondria and Energy Metabolism. The brain is one of the most metabolically expensive organs in the vertebrate body and large brains are, therefore, an evolutionarily costly adaptation (77). Tissues with high energy requirements, such as the brain, are highly dependent on mitochondria with hundreds to thousands within a single neuron (78). Signatures of adaptive evolution in nuclear-encoded mitochondrial genes have been found in large-brained/encephalized mammals including the elephant and anthropoid primates generally (79–81), as well as in bats, which have a high energy demand owing to flight (82). Mitochondria also play many important roles in the nervous system including in neurotransmitter metabolism, neurogenesis, neuroplasticity, and nervous system development and are strongly implicated in aging (83, 84). We find recurrent signatures of selection on the mitochondrion in multiple cebid lineages. This signature is the strongest in ancestral Cebinae with recurrent signatures across many annotation categories in the BM gene set including specific enriched terms related to the mitochondrial inner membrane and protein complexes which underlie the role of the mitochondrion as the cell's powerhouse. The ancestral capuchin branch is where absolute brain volume shows both the greatest total increase and the fastest rate of increase among Cebidae branches (30), supporting the putative relationship between this signature, encephalization, and the high energy requirements of large brains.

We also recover enriched broad mitochondrial terms for across-capuchins and ancestral Cebidae shared with the ancestral Cebinae branch, as well as additional signatures shared between across-capuchins and squirrel monkeys specific to nuclear-encoded mitochondrial ribosomal proteins (which form mitoribosomes) and the translation of essential mitochondrial messenger RNAs (mRNAs). Although signatures are sometimes shared across lineages, the genes involved usually differ; for example, there are four and six nuclear-encoded mitochondrial ribosomal genes for the across-capuchins and squirrel monkey branches, respectively, but with no overlapping genes. These results further support an evolutionary history of encephalization initiating in ancestral Cebidae and continuing independently in capuchins and squirrel monkeys.

Longevity, Aging, and Neurodegeneration. If large brains provide cognitive advantages that lead to, for example, reduced predation risk by outsmarting predators, or buffering from mortality due to food scarcity through tool-use abilities, large brains may

have an adaptive impact by reducing mortality thereby allowing selection to favor a longer life (85–87). In this regard, the parallels between humans and capuchins are striking: Capuchin monkeys have slow maturation and extended juvenescence reaching maturity at around 8 to 10 y old. Capuchin monkeys are among the most-long-lived primates, reaching over 50 y in captivity, though life expectancy is thought to be much lower in the wild (88, 89). Consistent with this, we recovered broad signatures of selection on aging and related processes across various capuchin branches.

The maintenance of genomic stability is considered a major factor underlying human longevity, with the accumulation of macromolecular damage, such as DNA damage, one of the most significant factors contributing to aging (90). We recover signatures of selection on DNA damage and repair-related genes for both the robust and gracile capuchin branches independently, including enriched terms such as “double strand break repair,” “cellular response to DNA damage stimulus,” “DNA repair,” and “DNA damage.” These results support those of Orkin et al. (49), who also found signatures of selection related to DNA repair and damage in *C. imitator*. Aging is also associated with a decline in mitochondrial function with strong links between mitochondria and a wide range of processes associated with aging including senescence and inflammation (84). As discussed in a previous section, there are strong signatures of selection on mitochondria across cebid branches.

Squirrel monkeys are also long-lived primates when considering their small body size—around 30 y in captivity (88)—and thus selective pressure on longevity may have arisen along the ancestral Cebidae branch. Indeed, for ancestral Cebidae we found the enriched disease annotation “aging” with several genes implicated in age-related neurodegeneration. A particularly notable gene in this annotation is *WRN*, which plays a major role in genome stability, with mutations in *WRN* associated with defective telomere maintenance and causing Werner syndrome, which is characterized by rapid onset of cellular senescence, early cancer onset, and premature aging (91). In addition, there are several important genes with signatures of selection related to sphingolipid and ceramide metabolism for ancestral Cebidae including a ceramide synthase (*CERS4*) and *SMPD1*, which encodes a lysosomal acid sphingomyelinase. Recent studies have highlighted the importance of acid sphingomyelinase as a critical mediator for pathologies in aging and age-related neurodegenerative diseases, with acid sphingomyelinase viewed as a promising drug target for antiaging and the treatment of age-related neurodegenerative diseases (92). We also find another important ceramide synthase gene, *CERS*, in the across-capuchin gene set, which catalyzes the synthesis of C18-ceramide in brain neurons, with elevated expression of this gene associated with increased longevity in humans (93).

Humans are particularly susceptible to age-related neurodegenerative disorders such as Alzheimer’s disease. While non-human primates show some age-related neurodegeneration, pathological neurodegeneration such as seen in Alzheimer’s disease is uncommon (94). Interestingly, we recover many genes across the capuchin branches associated with age-related neurodegenerative disorders in humans. This is particularly evident for robust capuchins with various enriched disease annotations related to Alzheimer’s disease (also found for squirrel monkeys) and dementia, as well as several genes directly associated with Alzheimer’s disease including *APOE*, a major genetic risk factor locus in humans. For ancestral Cebidae, we recovered the important related gene *ADAM10*, an alpha secretase involved in the cleavage of APP, thereby preventing the generation of

amyloid beta peptides associated with the development of Alzheimer’s disease (95).

Notably, there is a strong relationship between circadian rhythms and aging. Emerging in early infancy, the circadian system undergoes significant changes through an organism’s lifespan affecting rhythms of behaviors, temperature regulation, and hormone release, among others, and is implicated in human longevity (96). We found signatures of selection on circadian rhythms in both ancestral Cebinae and across-capuchins represented by enriched BP GO terms and UP keywords and including genes encoding core components of the circadian clock such as *PER3*. Precisely timed rhythmic activities that are tuned to periodic biotic and abiotic cycles of an organism’s environment are likely to confer adaptive advantage (97) and these signatures may relate to a variety of factors including, for example, the high activity levels of capuchins, as well as capuchin longevity, slow maturation, and/or delayed life history.

Reproduction and Mating Systems. Platyrrhine primates show a diverse range of mating systems and sexual/reproductive characteristics and behaviors. Both capuchin and squirrel monkeys are characterized by multimale multifemale mating systems (polygynandry), unlike many of their closely related lineages, for example, the flexible polyandry–monogamy seen in callitrichids and the social monogamy of owl monkeys. Polygynandrous mating systems are associated with postcopulatory sexual selection through sperm competition (98). Sperm competition can be directed at the quantity and quality of sperm, for example effectuated via changes to rates of spermatogenesis, sperm cell size, morphology, and mobility, copulation frequency, testes size, and the morphology of the penis, accessory glands, and ducts (98). In line with the reproductive shift to polygynandry in ancestral Cebidae, we find strong signatures of selection putatively related to sperm competition in both gene sets with various enriched terms describing motile cilium and flagella, spermatogenesis, sperm development, male meiosis, fertilization, and reproduction. These terms cover a suite of interesting genes including two important members of the CatSper complex, a sperm-specific ion channel involved in several important steps of fertilization including sperm hyperactivation and capacitation, which allow sperm to reach and interact with an oocyte. Similar signatures can also be found for ancestral Cebinae with “fertilization” forming the top-ranked individual BP GO term, as well as more broadly on motile cilia. In line with the shift to multimale multifemale mating systems, cebid lineages are also characterized by larger group sizes, which is particularly notable for squirrel monkeys (99) and may underlie some of the enriched immune system–related results recovered for ancestral Cebidae, squirrel monkeys, and ancestral Cebinae.

The behavioral repertoire of capuchins includes new reproductive/courtship behaviors and complex intimate individual relationships, which may also relate to their mating system (100). In agreement, we recovered genes related to sex steroids and reproductive hormones/peptides in the ancestral Cebinae and across-capuchins gene sets. For across-capuchins, we also recovered enriched GO terms describing the secretion of gonadotropin, luteinizing hormone, and endocrine hormones. Several genes in these terms are involved in sex steroid metabolism, while others are associated with the pituitary glycoprotein hormones and prolactin such as *PRLH*, prolactin-releasing hormone, which stimulates prolactin release and regulates prolactin expression, as well as lactation, behavior, and the reproductive system. Among the most notable genes recovered for capuchins is *NPVF*, found in both the ancestral Cebinae and across-capuchins branches,

encoding the neuropeptides NPSF and NPVF (also referred to as the RFamide-related peptides, RFRP-1 and RFRP-3), which are mammalian homologs of the avian neuropeptide gonadotropin-inhibitory hormone. These neuropeptides act as potent negative regulators of gonadotropin synthesis and secretion, with a range of functions in the modulation of reproduction including the regulation of sexual behavior, sexual maturation, ovulatory cycle, gonadal function, reproductive seasonality, and stress-induced reproductive suppression, among others (101).

Body Size and Morphology. While the two capuchin lineages, robust and gracile, share many traits as discussed throughout, significant derived characters arose since their divergence 5 to 6 Ma, hence their division into two genera, *Sapajus* and *Cebus* (34, 102). The most notable differences relate to their body shape and skeletal morphology, and this is reflected in the strongest signatures of selection recovered individually for both lineages. In line with their name, robust capuchins (*Sapajus*) are generally stockier and more skeletally robust, with shorter, thicker limbs, as well as striking differences in craniodental morphology, particularly relating to the robust masticatory architecture of the skull, a specialization to process tougher foods (durophagy) such as encased nuts and palm fruits (34, 103). Further, *S. libidinosus* is known to habitually use stone tools to access a variety of encased foods including otherwise inaccessible foods, a skill that takes many years to perfect, and this ability likely relates to their more robust skeletal morphology (102, 104). This derived morphology is reflected in the range of enriched GO terms and candidate genes we found in this lineage related to facial, skeletal system, and skeletal muscle tissue morphogenesis and development, as well as BMP signaling pathway. Several genes in these terms are explicitly associated with skull bone fusion and morphology such as *SIX4*, *RAB23*, and *NIPBL*, which encodes the protein delangin that plays a role in the development of the limbs and skull/face bones (105–107).

Similarly, for gracile capuchins (*Cebus*)—characterized by long, slender limbs and a slither body plan (34, 38)—we recovered various enriched annotated terms related to limb and skeletal system development, including several homeobox transcription factors of the Hox (5 of 21 analyzed) and Shox (1 of 2 analyzed) families that play fundamental roles in embryonic pattern formation, axis control, and are required for normal limb development (108). Many other genes in these terms are also associated with various skeletal dysmorphologies and congenital limb defects in humans. More broadly, there are signatures of selection on embryonic development for gracile capuchins including enriched terms such as the GO term “chordate embryonic development” and UP keyword “developmental protein.” Taken together, the results for robust and gracile capuchins are suggestive of adaptive pressure on developmental pathways related to the skull/face, limbs, and skeletal system that may underlie the morphological differences between these capuchin lineages. Also related to morphology, we recover enriched the GO term “embryonic digit morphogenesis” for ancestral Cebinae. Capuchins have a high degree of manual dexterity, possessing pseudo-opposable thumbs augmenting their precision grip ability, which plays a role in their sensorimotor intelligence, and show increased dexterity compared to squirrel monkeys (109, 110).

Among the most unusual aspects of squirrel monkey biology is their large brain size in the context of their overall small body size, which distinguishes them from the other most encephalized primate lineages. Reconstructions have indicated that squirrel monkey body size decreased and their brain size increased further after squirrel monkeys and capuchins diverged

(30). Our results for squirrel monkeys reveal broad signatures related to growth factors across our analyses with enriched growth factor–related GO terms and genes encoding or associated with members of the fibroblast growth factor and transforming growth factor beta families and many implicated in human stature and dwarfism, including the short stature homeobox gene (*SHOX*). The strongest selective signatures for squirrel monkeys relate to cellular signaling cascades, with various enriched annotations describing the mitogen-activated protein kinase (MAPK) and ERK1/2 signaling pathways involved in basic cellular processes including cell proliferation and differentiation. Together, the signatures of selection on ERK/MAPK cascades and growth factors may be related to the reduced body size of squirrel monkeys and/or the adaptive maintenance of a large brain size while reducing body size.

Diet and Nutrition. Capuchins inhabit a complex omnivorous dietary niche characterized by dietary flexibility, high nutrient density, and easy digestibility for their small gut (111), with high sensorimotor intelligence related to their extractive foraging capabilities. For across-capuchins, we recovered various diet/metabolism-related signatures including for branched-chain amino acids, essential amino acids required in the diet that are major constituents of muscle protein; riboflavin, a B vitamin involved in many physiologic processes, necessary for normal cell growth and function; and biotin, another essential B vitamin involved in the conversion of food to energy and important for embryonic growth. It is notable that all of these nutrients are found in lipid- and protein-rich food sources such as meats, eggs, and nuts. Among the capuchin lineages, robust capuchins show a preference for food with a high lipid content such as nuts and insects (112), and we recover various enriched GO terms related to lipid metabolism, which may be linked to their increased ability (versus gracile capuchins) to access fat-rich nuts as a result of both their robust skeletal morphology and, in some species, their stone tool use. Robust capuchins also show various signatures potentially related to water homeostasis including enriched GO terms for kidney/renal system development and sodium ion transport. Selective pressure on water homeostasis may relate to range expansion into drier habitats such as the Cerrado for some *Sapajus* lineages in the Pleistocene (43).

Similarly, in the highly insectivorous squirrel monkeys (47) we recovered various enriched terms related to nutrition including mineral absorption, response to metal ions, retinoid metabolism, and calcium homeostasis, which is notable given many insects are considered a poor source of calcium.

Limitations and Future Directions. While a single genome per species or lineage can give insight into evolutionary processes deep in time, the sequencing of more individuals in each of these lineages will be critical for studying patterns of demography and selection in more recent history. The inclusion of additional individuals is also required to determine if variants discovered in this study are fixed or vary within species. Moreover, without functional genomic experiments, some of the candidate genes described in this study might reflect the relaxation of selection rather than adaptive evolution, and these genes thus remain candidates until they are validated. Furthermore, given that protein function, which is generally derived from humans, mice, and other model organisms, is little understood in the context of the biology of these cebid lineages, the functional significance of selection on these candidate genes and the association of these signals with specific adaptive functions is correlative and warrants further investigation. Codon-based

models of evolution are also unable to consider variation in regulatory controls and gene expression, which can both have important adaptive implications.

The draft reference assembly, short-read data, and RNAseq data from 17 tissues for the same robust capuchin individual provide a useful resource for future genomics studies of capuchins and primates more broadly. Future directions might include long-read sequencing, a candidate technology to fill gaps in the assembly and increase the contiguity to chromosome scale. The results from this study will be useful in downstream applications for the study of genes of interest in both captive and field studies of platyrrhines, as well as opening new avenues of research for the study of primate brain evolution and comparative brain biology.

Materials and Methods

Genome Sequencing, Assembly, and Size Estimation. Whole blood was collected during a routine physical from Mango, a female captive brown robust capuchin (*S. apella*) housed at the Language Research Center, Georgia State University (Institutional Animal Care and Use Committee number: A16031). Mango was aged and thought to have been wild-caught in the 1970s, and she was the last remaining individual from the colony's original source population. Dovetail Genomics extracted high-molecular-weight DNA from the blood sample to construct one shotgun library and three "Chicago" proximity ligation libraries with chimeric pairs spanning up to 50 kbp in physical distance. The shotgun library was sequenced across four HiSeq. 4000 lanes, producing 1.33 billion 150-bp paired end (PE) read pairs (399 Gbp), an estimated 148-fold sequencing coverage (based on a genome size of 2.7 Gbp). The three Chicago libraries were pooled and sequenced across two HiSeq. 4000 lanes, generating 800 million 100-bp PE read pairs with ~220-fold physical coverage. All sequencing was performed at the DNA Technologies Core, University of California, Davis. All raw reads were deposited on NCBI's sequence read archive (SRA) (SI Appendix, Table S1). A preliminary de novo assembly was generated by Dovetail Genomics from quality-filtered short-read shotgun data using the Meraculous assembler (113). The final draft assembly was generated by scaffolding the preliminary assembly with the Chicago libraries using Dovetail's HiRise pipeline (51). Total length of this genome assembly was 2,520.3 Mbp (in 6,631 scaffolds) with an N50 of 27.1 Mbp (29 scaffolds) and N90 of 4.04 Mbp (116 scaffolds). The longest scaffold was 90.4 Mbp.

We evaluated completeness of the genome assembly by its estimated gene content using CEGMA v2.5 (53) and BUSCO v3.0.2 (52) to calculate the proportion of 248 CEGs or 6,192 Euarctontoglires-specific conserved single-copy orthologs, respectively, that were either complete, fragmented, or missing. Using quality-filtered, nuclear-only, endogenous short reads, we also performed *k*-mer counting with Jellyfish v.2.2.6 (114) to generate a *k*-mer frequency distribution of 31-mers and then estimated genome size using four approaches. We generated an initial mitochondrial genome assembly for Mango by mapping a set of putative mitochondrial short read pairs to a complete *S. apella* mitochondrial genome using MIRA v.4.0.2 (115) and then performed baiting and iterative mapping with a MITObim v.1.9.1 (116) wrapper script to generate the final mitochondrial genome assembly.

RNAseq and Transcript Assemblies. The reference individual, Mango, was killed in the months after genome sequencing when her health declined and a cancerous tumor was discovered, allowing the ethical collection of fresh tissue for RNA sequencing from the same individual. Tissue collection was performed during necropsy at Yerkes National Primate Research Center within hours of her death. Seventeen tissues samples were harvested and placed in RNAlater (Invitrogen), and subsequently total RNA was isolated from each sample followed by poly-A tail selection library preparation. The libraries were pooled and sequenced on a single HiSeq. 3000 lane generating ~367 million 150-bp PE read pairs (102.5 Gbp) with between 16.8 and 27.4 million reads pairs per tissue. These steps were performed by the Technology Center for Genomics & Bioinformatics (TCGB) at the University of California, Los Angeles (UCLA). All raw reads were deposited on NCBI's SRA (SI Appendix, Table S1). After *k*-mer correction, filtering, trimming, and ribosomal RNA removal steps, we generated seven transcript assemblies with the cleaned RNAseq read pairs, as follows: de novo (TrinDNv2);

abundance-filtered de novo (TrinDNv2); reference-based (Cuffv1); PASA with TrinDNv2 and Cuffv1 as input (PASAv1); genome-guided (TrinGGv1); PASA with TrinDNv2, Cuffv1, and TrinGGv1 as input (PASAv2); and nonredundant with PASAv2 as input (NRv1). This ultimately resulted in three assemblies (TrinDNv2, PASAv1, and NRv1) for use as direct evidence in various iterations of the genome annotation pipeline. We checked quality metrics and completeness of the seven assemblies using rnaQUAST v1.5.0 (55) with BUSCO v3.0.2 in transcriptome mode using the Euarctontoglires-specific BUSCOs gene set.

Repeat and Genome Annotation. To assess the repeat content of the robust capuchin genome, we first performed a homology-based repeat annotation of our genome assembly using known elements with RepeatMasker v4.0.7 (117), followed by de novo repeat identification using the library of unknown repeats generated with RepeatModeler v1.0.11 (118), and finally we used ProcessRepeats from RepeatMasker to summarize all annotated repeats in the genome assembly. We annotated the robust capuchin genome assembly in three iterations of Maker v3.01.02 (56, 57) to predict gene models, incorporating direct evidence from transcript assemblies, homology to the predicted proteomes of platyrrhine primates and humans, and ab initio predictions from Augustus v3.3 (119) with a robust capuchin-specific hidden Markov model that was trained initially in BUSCO and twice subsequently using high-quality gene models from each of the first two passes of Maker (SI Appendix, Table S6). Predicted gene models from the third pass of Maker were functionally annotated using Blast2GO v5.2.5 (120) and filtered based on supporting evidence and presence of annotations.

Identification of Orthologs, Alignment, and Filtering. In order to assess signatures of positive selection in other platyrrhine primate genomes, we first identified orthologs using the OrthoMCL pipeline (121) across 10 species: four platyrrhine primates (*Sapajus*, *Cebus*, *Saimiri*, and *Callithrix*), five other primates (*Macaca*, *Pan*, *Homo*, *Carlito*, and *Microcebus*), and mouse (*Mus*). As input to the pipeline, we used predicted CDS and protein sequence files from Ensembl (or for *Sapajus* from our genome annotation) for all species that were filtered for the longest isoform per gene. We generated a set of 9,216 conservative, manually curated CDS alignments which were highly likely to represent one-to-one orthologs across their length by 1) filtering the OrthoMCL output for one-to-one orthologs, a minimum of five species, and the presence of at least one capuchin lineage; 2) aligning CDS sequences for these filtered orthologs groups by codon using Guidance2 v.2.02 (58) with the MAFFT aligner v.7.419 (122) with 100 guidance bootstraps; and 3) visually inspecting all alignments for errors and editing as required to reduce the likelihood of false positives.

BM and BSM tests. We specified six lineages (foreground branches) for the positive selection tests, as follows: H1, robust capuchin (*Sapajus*); H2, gracile capuchin (*Cebus*); H3, ancestral Cebinae (capuchins); H3a, across-capuchins more generally (all Cebinae); H4, ancestral Cebidae; and H5, squirrel monkey (*Saimiri*). We assigned species set IDs to each combination of species (207 species sets) found in the final alignments and generated unrooted tree files based on the consensus species tree (Fig. 1) that specified the various foreground branches analyzed for each species set (759 tree files). We ran two different tests for positive selection with codeml from the PAML package v.4.9 (59) which are based on rates of nonsynonymous versus synonymous substitutions (ω or dN/dS ratio): the BSM, which tests for episodic selection by searching for positively selected sites in the foreground branch, and the BM, which tests for elevated dN/dS ratios along the foreground branch indicating accelerated evolution. We did not run the BSM test for H3a, and thus a total of 11 lineage and test combinations were conducted with codeml. For each BM test, we assessed two models as follows: the alternative branch model which separates the tree into foreground and background branches that have distinct ω parameters allowing them to evolve with separate dN/dS ratios and the null model which uses a single ω parameter across the tree. For each BSM test, we assessed an alternative BSM allowing for positive selection on the foreground branch and a null model allowing only for purifying and neutral selection on the foreground and background lineages. After estimating parameters and calculating the likelihood with codeml, we performed LRTs by comparing the likelihood of the alignment under the alternative versus under the null model and calculated *P* values from the χ^2 distribution with one degree of freedom.

We used the Benjamini-Hochberg method (123) to correct for multiple testing, applying a single level of correction within each foreground branch for each test by controlling the FDR. Even using a low FDR-corrected *P* value there were no or very few (five or fewer) significant genes after correction for all BSM tests and most lineages for BM tests. We consider the overall set of significant genes according to uncorrected *P* values (<0.05) to be the most likely set of genome-wide candidates from the background set for each lineage and refer to these sets of genes as candidate adaptively evolving genes. We conducted gene set enrichment analyses on the set of candidate adaptively evolving genes, one for each lineage and test (BM or BSM; 11 total) using DAVID v.6.8 (60) with the entire human gene set as the background population of genes. In DAVID, we assessed lists/charts of enriched 1) BP, CC, and MF GO terms (the "all" option), 2) UP keywords, 3) KEGG pathways, 4) Reactome pathways, and 5) disease annotations, as well as functional annotation clustering across the three GO terms together under the high classification stringency criteria, with an EASE score of <0.05 required for all enriched annotated terms for both approaches and a minimum enrichment score of 1.3 for the annotation clusters.

Data, Materials, and Software Availability. The reference genome (https://www.ncbi.nlm.nih.gov/assembly/GCA_022120495.1) (124), and whole-genome, Chicago library, and RNA sequencing reads (https://www.ncbi.nlm.nih.gov/sra?linkname=bioproject_sra_all&from_uid=717806) for our reference *S. apella* individual are publicly available at NCBI (BioProjects accession PRJNA717806) (<https://www.ncbi.nlm.nih.gov/bioproject?term=PRJNA717806>) (125). See *SI Appendix, Table S1* for NCBI's SRA accessions for the raw short-read

data for the shotgun and Chicago libraries. The version of the reference genome assembly used in this study, as well as the mitochondrial genome assembly and annotation, are available in a Zenodo repository (https://zenodo.org/record/5225106#_YuwD7RzMJPY) (126).

ACKNOWLEDGMENTS. We thank Jonathon Rodgers and LSSA Support at UCLA for computational assistance; staff at Dovetail Genomics, DNA Technologies Core (University of California, Davis), and TCGB (UCLA) for sequencing assistance; Amelia Wilkes and the staff at the Language Research Center for Mango's care and the collection of her blood sample; staff at Yerkes National Primate Research Center for tissue collection for RNAseq during Mango's necropsy; the Broad Institute, Amanda Melin, and Joe Orkin for generating the squirrel monkey and gracile capuchin genomes used in this study; Stephen Nash for the use of his illustrations; Colin Brand for his helpful comments; and the Institute for Society and Genetics (UCLA) and Anthropology Department (University of Utah) for post-doctoral support for H.B. This work was supported by Fundação de Amparo à Pesquisa do Estado de São Paulo grant 14/13237-1 (Principal Investigator, J.W.L.) and start-up funding from the University of Utah (T.H.W.).

Author affiliations: ^aDepartment of Anthropology, University of Utah, Salt Lake City, UT 84112; ^bInstitute for Society and Genetics, University of California, Los Angeles, CA 90095; ^cLanguage Research Center, Department of Psychology, Center for Behavioral Neuroscience, Georgia State University, Atlanta, GA 30302; ^dDepartment of Experimental Psychology, University of São Paulo, São Paulo 05508-060, Brazil; and ^eDepartment of Anthropology, University of California, Los Angeles, CA 90095

- R. Hoffstetter, R. Lavocat, Découverte dans le Déséadien de Bolivie de genres pentalophodontes appuyant les affinités africaines des Rongeurs Caviomorpes. *C.R. Acad. Sci.* **273**, 2215-2218 (1970).
- W. C. Hartwig, "Patterns, puzzles and perspectives on platyrrhine origins" in *Integrative Paths to the Past: Paleoanthropological Advances in Honor of F. Clark Howell*, R. S. Corruccini, R. L. Ciochon, Eds. (Prentice Hall, 1994), pp. 69-94.
- A. Houle, The origin of platyrrhines: An evaluation of the Antarctic scenario and the floating island model. *Am. J. Phys. Anthropol.* **109**, 541-559 (1999).
- P. Perelman *et al.*, A molecular phylogeny of living primates. *PLoS Genet.* **7**, e1001342 (2011).
- M. S. Springer *et al.*, Macroevolutionary dynamics and historical biogeography of primate diversification inferred from a species supermatrix. *PLoS One* **7**, e49521 (2012).
- M. Bond *et al.*, Eocene primates of South America and the African origins of New World monkeys. *Nature* **520**, 538-541 (2015).
- R. Hoffstetter, Un Primate de l'Oligocène inférieur sud-américain: *Branisella boliviana* gen. et sp. nov. *C. R. Acad. Sci. Paris* **269**, 434-437 (1969).
- A. L. Rosenberger, T. Setoguchi, W. C. Hartwig, *Laurentia annectens*, new genus and species: fossil evidence for the origins of callitrichine New World monkeys. *Proc. Natl. Acad. Sci. U.S.A.* **88**, 2137-2140 (1991).
- M. Takai, F. Anaya, N. Shigehara, T. Setoguchi, New fossil materials of the earliest new world monkey, *Branisella boliviana*, and the problem of platyrrhine origins. *Am. J. Phys. Anthropol.* **111**, 263-281 (2000).
- R. F. Kay, Biogeography in deep time - What do phylogenetics, geology, and paleoclimate tell us about early platyrrhine evolution? *Mol. Phylogenet. Evol.* **82** (Pt B), 358-374 (2015).
- L. Marivaux *et al.*, Neotropics provide insights into the emergence of New World monkeys: New dental evidence from the late Oligocene of Peruvian Amazonia. *J. Hum. Evol.* **97**, 159-175 (2016).
- A. L. Rosenberger, "Platyrrhine paleontology and systematics: the paradigm shifts" in *The Primate Fossil Record*, W. C. Hartwig, Ed. (Cambridge University Press, 2002), pp. 151-160.
- A. L. Rosenberger, Evolutionary morphology, platyrrhine evolution, and systematics. *Anat. Rec. (Hoboken)* **294**, 1955-1974 (2011).
- M. F. Tejedor, Sistemática, evolución y paleobiogeografía de los primates *Platyrrhini*. *Rev. del Mus. la Plata* **20**, 20-39 (2013).
- J. A. Hodgson *et al.*, Successive radiations, not stasis, in the South American primate fauna. *Proc. Natl. Acad. Sci. U.S.A.* **106**, 5534-5539 (2009).
- X. Wang *et al.*, Reconstructing the phylogeny of new world monkeys (*Platyrrhini*): Evidence from multiple non-coding loci. *Curr. Zool.* **65**, 579-588 (2019).
- J. Cracraft *et al.*, "The origin and evolution of Amazonian species diversity" in *Neotropical Diversification: Patterns and Processes*, V. Rull, A. Carnaval, Eds. (Springer, 2020), pp. 225-244.
- J. G. Fleagle, *Primate Adaptation and Evolution* (Academic Press, 2013).
- N. M. Jameson Kiesling, S. V. Yi, K. Xu, F. Gianluca Sperone, D. E. Wildman, The tempo and mode of New World monkey evolution and biogeography in the context of phylogenomic analysis. *Mol. Phylogenet. Evol.* **82** (Pt B), 386-399 (2015).
- A. Rylands, R. A. Mittermeier, "Family Cebidae (capuchins and squirrel monkeys)" in *Handbook of the Mammals of the World*, R. Mittermeier, A. B. Rylands, D. E. Wilson, Eds. (Lynx Edicions, 2013), vol. 3, pp. 348-389.
- A. Estrada *et al.*, Primates in peril: The significance of Brazil, Madagascar, Indonesia and the Democratic Republic of the Congo for global primate conservation. *PeerJ* **6**, e4869 (2018).
- W. C. Hartwig, D. J. Meldrum, "Miocene platyrrhines of the northern Neotropics" in *The Primate Fossil*, W. C. Hartwig, Ed. (Cambridge University Press, 2002), pp. 175-188.
- J. L. Alfaro, The monkeying of the Americas: Primate biogeography in the Neotropics. *Annu. Rev. Anthropol.* **46**, 317-336 (2017).
- L. M. Valencia, A. Martins, E. M. Ortiz, A. Di Fiore, A RAD-sequencing approach to genome-wide marker discovery, genotyping, and phylogenetic inference in a diverse radiation of primates. *PLoS One* **13**, e0201254 (2018).
- K. L. Chiou, L. Pozzi, J. W. Lynch Alfaro, A. Di Fiore, Pleistocene diversification of living squirrel monkeys (*Saimiri* spp.) inferred from complete mitochondrial genome sequences. *Mol. Phylogenet. Evol.* **59**, 736-745 (2011).
- R. A. Stirton, Ceboid monkeys from the Miocene of Colombia. *Univ. Calif. Publ. Geol. Sci.* **28**, 315-335 (1951).
- M. Takai, New specimens of *Neosaimiri fieldsi* from La Venta, Colombia: A middle Miocene ancestor of the living squirrel monkeys. *J. Hum. Evol.* **27**, 329-360 (1994).
- T. Setoguchi, M. Takai, N. Shigehara, A new ceboid primate, closely related to *Neosaimiri*, found in the upper red bed in the La Venta Badlands, Middle Miocene of Colombia, South America. *Kyoto Univ. Overseas Res. Reports New World Monkeys*, **7**, 9-13 (1990).
- R. F. Kay, D. J. Meldrum, "A new small platyrrhine from the Miocene of Colombia and the phyletic position of Callitrichinae" in *Vertebrate Paleontology in the Neotropics*, R. F. Kay, R. H. Madden, R. L. Cifelli, J. J. Flynn, Eds. (Smithsonian Institution Press, 1997), pp. 435-458.
- S. H. Montgomery, I. Capellini, R. A. Barton, N. I. Mundy, Reconstructing the ups and downs of primate brain evolution: Implications for adaptive hypotheses and *Homo floresiensis*. *BMC Biol.* **8**, 9 (2010).
- D. M. Fragaszy, E. Visalberghi, L. M. Fedigan, *The Complete Capuchin: The Biology of the Genus Cebus* (Cambridge University Press, 2004).
- A. L. Rosenberger, Gradistic views and adaptive radiation of platyrrhine primates. *Z. Morphol. Anthropol.* **71**, 157-163 (1980).
- G. Marroig, When size makes a difference: Allometry, life-history and morphological evolution of capuchins (*Cebus*) and squirrels (*Saimiri*) monkeys (Cebinae, Platyrrhini). *BMC Evol. Biol.* **7**, 20 (2007).
- J. W. Alfaro, J. D. Silva Jr., A. B. Rylands, How different are robust and gracile capuchin monkeys? An argument for the use of *Sapajus* and *Cebus*. *Am. J. Primatol.* **74**, 273-286 (2012).
- E. B. Ottoni, P. Izar, Capuchin monkey tool use: Overview and implications. *Evol. Anthropol.* **17**, 171-178 (2008).
- S. Perry *et al.*, Social conventions in wild white-faced capuchin monkeys: Evidence for traditions in a neotropical primate. *Curr. Anthropol.* **44**, 241-268 (2003).
- S. M. Ford, R. S. Corruccini, "Intraspecific, interspecific, metabolic, and phylogenetic scaling in platyrrhine primates" in *Size and Scaling in Primate Biology*, W. L. Jungers, Ed. (Plenum Press, 1985), pp. 401-435.
- W. L. Jungers, J. G. Fleagle, Postnatal growth allometry of the extremities in *Cebus albifrons* and *Cebus apella*: A longitudinal and comparative study. *Am. J. Phys. Anthropol.* **53**, 471-478 (1980).
- M. Bouvier, Biomechanical scaling of mandibular dimensions in New World monkeys. *Int. J. Primatol.* **7**, 551-567 (1986).
- C. D. Byron, Cranial suture morphology and its relationship to diet in *Cebus*. *J. Hum. Evol.* **57**, 649-655 (2009).
- J. W. Lynch Alfaro *et al.*, Explosive Pleistocene range expansion leads to widespread Amazonian sympatry between robust and gracile capuchin monkeys. *J. Biogeogr.* **39**, 272-288 (2012).
- M. G. M. Lima *et al.*, A phylogenomic perspective on the robust capuchin monkey (*Sapajus*) radiation: First evidence for extensive population admixture across South America. *Mol. Phylogenet. Evol.* **124**, 137-150 (2018).
- M. G. M. Lima *et al.*, Capuchin monkey biogeography: Understanding *Sapajus* Pleistocene range expansion and the current sympatry between *Cebus* and *Sapajus*. *J. Biogeogr.* **44**, 810-820 (2017).
- R. F. Kay, M. A. Cuzzo, New platyrrhine monkeys from the Solimões Formation (late Miocene, Acre State, Brazil). *J. Hum. Evol.* **50**, 673-686 (2006).
- F. R. Negri, J. B. B. Quentim-Villanueva, J. Ferigolo, P.-O. Antoine, "A review of Tertiary mammal faunas and birds from western Amazonia" in *Amazonia: Landscape and Species Evolution: A Look into the Past*, C. Hoorn, Ed. (Blackwell Publishing, 2009), pp. 245-258.
- J. Royo, S. J. Forkel, P. Pouget, M. Thiebaut de Schotten, The squirrel monkey model in clinical neuroscience. *Neurosci. Biobehav. Rev.* **128**, 152-164 (2021).

47. H. S. Zimble-Delorenzo, A. I. Stone, Integration of field and captive studies for understanding the behavioral ecology of the squirrel monkey (*Saimiri* sp.). *Am. J. Primatol.* **73**, 607–622 (2011).
48. S. D. Tardif, C. R. Abbee, K. G. Mansfield, Workshop summary: Neotropical primates in biomedical research. *ILAR J.* **52**, 386–392 (2011).
49. J. D. Orkin *et al.*, The genomics of ecological flexibility, large brains, and long lives in capuchin monkeys revealed with fecalFACS. *Proc. Natl. Acad. Sci. U.S.A.* **118**, e2010632118 (2021).
50. A. M. Boddy *et al.*, Evidence of a conserved molecular response to selection for increased brain size in primates. *Genome Biol. Evol.* **9**, 700–713 (2017).
51. N. H. Putnam *et al.*, Chromosome-scale shotgun assembly using an in vitro method for long-range linkage. *Genome Res.* **26**, 342–350 (2016).
52. F. A. Simão, R. M. Waterhouse, P. Ioannidis, E. V. Kriventseva, E. M. Zdobnov, BUSCO: Assessing genome assembly and annotation completeness with single-copy orthologs. *Bioinformatics* **31**, 3210–3212 (2015).
53. G. Parra, K. Bradnam, I. Korf, CEGMA: A pipeline to accurately annotate core genes in eukaryotic genomes. *Bioinformatics* **23**, 1061–1067 (2007).
54. L. Fantini, M. D. Mudry, M. Nieves, Genome size of two *Cebus* species (primates: *platyrrhini*) with a fertile hybrid and their quantitative genomic differences. *Cytogenet. Genome Res.* **135**, 33–41 (2011).
55. E. Bushmanova, D. Antipov, A. Lapidus, V. Suvorov, A. D. Prijbelski, maQUAST: A quality assessment tool for de novo transcriptome assemblies. *Bioinformatics* **32**, 2210–2212 (2016).
56. C. Holt, M. Yandell, MAKER2: An annotation pipeline and genome-database management tool for second-generation genome projects. *BMC Bioinformatics* **12**, 491 (2011).
57. M. S. Campbell *et al.*, MAKER-P: A tool kit for the rapid creation, management, and quality control of plant genome annotations. *Plant Physiol.* **164**, 513–524 (2014).
58. I. Sela, H. Ashkenazy, K. Katoh, T. Pupko, GUIDANCE2: Accurate detection of unreliable alignment regions accounting for the uncertainty of multiple parameters. *Nucleic Acids Res.* **43** (W1), W7–14 (2015).
59. Z. Yang, PAML 4: Phylogenetic analysis by maximum likelihood. *Mol. Biol. Evol.* **24**, 1586–1591 (2007).
60. W. Huang, B. T. Sherman, R. A. Lempicki, Systematic and integrative analysis of large gene lists using DAVID bioinformatics resources. *Nat. Protoc.* **4**, 44–57 (2009).
61. H. J. Jerison, Animal intelligence as encephalization. *Philos. Trans. R. Soc. Lond. B Biol. Sci.* **308**, 21–35 (1985).
62. M. Igarashi, Molecular basis of the functions of the mammalian neuronal growth cone revealed using new methods. *Proc. Jpn. Acad., Ser. B, Phys. Biol. Sci.* **95**, 358–377 (2019).
63. J. Guo *et al.*, Primary cilia signaling promotes axonal tract development and is disrupted in Joubert syndrome-related disorders models. *Dev. Cell* **51**, 759–774.e5 (2019).
64. S. M. Park, H. J. Jang, J. H. Lee, Roles of primary cilia in the developing brain. *Front. Cell Neurosci.* **13**, 218 (2019).
65. Y. Q. Wang *et al.*, Accelerated evolution of the pituitary adenylate cyclase-activating polypeptide precursor gene during human origin. *Genetics* **170**, 801–806 (2005).
66. H. Stephan, G. Baron, H. D. Frahm, Comparative size of brains and brain structures. *Comp. Primate Biol.* **4**, 1–38 (1988).
67. J. D. Sweatt, Neural plasticity and behavior – Sixty years of conceptual advances. *J. Neurochem.* **139** (suppl. 2), 179–199 (2016).
68. J. W. Fawcett, T. Oohashi, T. Pizzorosso, The roles of perineuronal nets and the perinodal extracellular matrix in neuronal function. *Nat. Rev. Neurosci.* **20**, 451–465 (2019).
69. A. C. Reichelt, D. J. Hare, T. J. Bussey, L. M. Saksida, Perineuronal nets: Plasticity, protection, and therapeutic potential. *Trends Neurosci.* **42**, 458–470 (2019).
70. E. Visalberghi *et al.*, Selection of effective stone tools by wild bearded capuchin monkeys. *Curr. Biol.* **19**, 213–217 (2009).
71. S. Perry, Social traditions and social learning in capuchin monkeys (*Cebus*). *Philos. Trans. R. Soc. Lond. B Biol. Sci.* **366**, 988–996 (2011).
72. S. Perry, Behavioural variation and learning across the lifespan in wild white-faced capuchin monkeys. *Philos. Trans. R. Soc. Lond. B Biol. Sci.* **375**, 20190494 (2020).
73. J. W. Smith, A. T. Evans, B. Costall, J. W. Smythe, Thyroid hormones, brain function and cognition: A brief review. *Neurosci. Biobehav. Rev.* **26**, 45–60 (2002).
74. M. Shimajo *et al.*, Synaptotagmin-11 mediates a vesicle trafficking pathway that is essential for development and synaptic plasticity. *Genes Dev.* **33**, 365–376 (2019).
75. M. A. Lancaster *et al.*, Defective Wnt-dependent cerebellar midline fusion in a mouse model of Joubert syndrome. *Nat. Med.* **17**, 726–731 (2011).
76. R. J. Ferland *et al.*, Abnormal cerebellar development and axonal decussation due to mutations in *AH11* in Joubert syndrome. *Nat. Genet.* **36**, 1008–1013 (2004).
77. J. W. Mink, R. J. Blumenschine, D. B. Adams, Ratio of central nervous system to body metabolism in vertebrates: Its constancy and functional basis. *Am. J. Physiol.* **241**, R203–R212 (1981).
78. M. Rango, N. Bresolin, Brain mitochondria, aging, and Parkinson's disease. *Genes (Basel)* **9**, 250 (2018).
79. J. W. Doan *et al.*, Coadaptive evolution in cytochrome c oxidase: 9 of 13 subunits show accelerated rates of nonsynonymous substitution in anthropoid primates. *Mol. Phylogenet. Evol.* **33**, 944–950 (2004).
80. L. I. Grossman, D. E. Wildman, T. R. Schmidt, M. Goodman, Accelerated evolution of the electron transport chain in anthropoid primates. *Trends Genet.* **20**, 578–585 (2004).
81. M. Goodman *et al.*, Phylogenomic analyses reveal convergent patterns of adaptive evolution in elephant and human ancestries. *Proc. Natl. Acad. Sci. U.S.A.* **106**, 20824–20829 (2009).
82. Y. Y. Shen *et al.*, Adaptive evolution of energy metabolism genes and the origin of flight in bats. *Proc. Natl. Acad. Sci. U.S.A.* **107**, 8666–8671 (2010).
83. A. Cheng, Y. Hou, M. P. Mattson, Mitochondria and neuroplasticity. *ASN Neuro* **2**, e00045 (2010).
84. N. Sun, R. J. Youle, T. Finkel, The mitochondrial basis of aging. *Mol. Cell* **61**, 654–666 (2016).
85. J. M. Allman, T. McLaughlin, A. Hakeem, Brain structures and life-span in primate species. *Proc. Natl. Acad. Sci. U.S.A.* **90**, 3559–3563 (1993).
86. C. González-Lagos, D. Sol, S. M. Reader, Large-brained mammals live longer. *J. Evol. Biol.* **23**, 1064–1074 (2010).
87. K. Isler, C. P. Van Schaik, How humans evolved large brains: Comparative evidence. *Evol. Anthropol.* **23**, 65–75 (2014).
88. C. P. van Schaik, K. Isler, "Life history evolution in primates" in *The Evolution of Primate Societies*, J. C. Mitani, J. Call, P. M. Kappeler, R. A. Palombit, J. B. Silk, Eds. (University of Chicago Press, 2012), pp. 220–244.
89. A. M. Bronikowski *et al.*, Female and male life tables for seven wild primate species. *Sci. Data* **3**, 160006 (2016).
90. M. Yousefzadeh *et al.*, DNA damage-how and why we age? *eLife* **10**, 1–17 (2021).
91. A. S. Multani, S. Chang, WRN at telomeres: Implications for aging and cancer. *J. Cell Sci.* **120**, 713–721 (2007).
92. M. H. Park, H. K. Jin, J. S. Bae, Potential therapeutic target for aging and age-related neurodegenerative diseases: The role of acid sphingomyelinase. *Exp. Mol. Med.* **52**, 380–389 (2020).
93. S. M. Jazwinski *et al.*; Georgia Centenarian Study and the Louisiana Healthy Aging Study, HRAS1 and LASS1 with APOE are associated with human longevity and healthy aging. *Aging Cell* **9**, 698–708 (2010).
94. A. Von Gunten, M. Therese Clerc, R. Tomar, P. S. John Smith, Evolutionary considerations on aging and Alzheimer's disease. *J. Alzheimer's Dis. Park.* **08**, 1–12 (2018).
95. S. Lammich *et al.*, Constitutive and regulated α -secretase cleavage of Alzheimer's amyloid precursor protein by a disintegrin metalloprotease. *Proc. Natl. Acad. Sci. U.S.A.* **96**, 3922–3927 (1999).
96. O. Froy, Circadian rhythms, aging, and life span in mammals. *Physiology (Bethesda)* **26**, 225–235 (2011).
97. D. A. Paranjpe, V. K. Sharma, Evolution of temporal order in living organisms. *J. Circadian Rhythms* **3**, 7 (2005).
98. A. F. Dixon, Copulatory and postcopulatory sexual selection in primates. *Folia Primatol. (Basel)* **89**, 258–286 (2018).
99. T. Pinheiro, S. F. Ferrari, M. A. Lopes, Activity budget, diet, and use of space by two groups of squirrel monkeys (*Saimiri sciureus*) in eastern Amazonia. *Primates* **54**, 301–308 (2013).
100. P. Izar, A. Stone, S. Carnegie, E. S. Nakai, "Sexual selection, female choice and mating systems" in *South American Primates: Comparative Perspectives in the Study of Behavior, Ecology, and Conservation*, A. P. Garber, A. Estrada, J. C. Bicca-Marques, E. W. Heymann, K. B. Strier, Eds. (Springer, 2009), pp. 157–189.
101. T. Ubuka, K. Tsutsui, Reproductive neuroendocrinology of mammalian gonadotropin-inhibitory hormone. *Reprod. Med. Biol.* **18**, 225–233 (2019).
102. K. A. Wright *et al.*, The effects of ecology and evolutionary history on robust capuchin morphological diversity. *Mol. Phylogenet. Evol.* **82** (Pt B), 455–466 (2015).
103. T. J. Masterson, Sexual dimorphism and interspecific cranial form in two capuchin species: *Cebus albifrons* and *C. apella*. *Am. J. Phys. Anthropol.* **104**, 487–511 (1997).
104. Y. Eschchar, P. Izar, E. Visalberghi, B. Resende, D. Fragaszy, When and where to practice: Social influences on the development of nut-cracking in bearded capuchins (*Sapajus libidinosus*). *Anim. Cogn.* **19**, 605–618 (2016).
105. N. Funato, New insights into cranial synchondrosis development: A mini review. *Front. Cell Dev. Biol.* **8**, 706 (2020).
106. M. R. Hasan *et al.*, RAB23 coordinates early osteogenesis by repressing FGF10-pERK1/2 and GLI1. *eLife* **9**, 1–26 (2020).
107. M. Ansari *et al.*, Genetic heterogeneity in Cornelia de Lange syndrome (CdLS) and CdLS-like phenotypes with observed and predicted levels of mosaicism. *J. Med. Genet.* **51**, 659–668 (2014).
108. C. McQueen, M. Towers, Establishing the pattern of the vertebrate limb. *Development* **147**, dev177956 (2020).
109. M. B. Costello, D. M. Fragaszy, Prehension in *Cebus* and *Saimiri*: I. Grip type and hand preference. *Am. J. Primatol.* **15**, 235–245 (1988).
110. V. Truppa, P. Carducci, G. Sabbatini, Object grasping and manipulation in capuchin monkeys (genera *Cebus* and *Sapajus*). *Biol. J. Linn. Soc. Lond.* **127**, 563–582 (2019).
111. K. L. Allen, R. F. Kay, Dietary quality and encephalization in platyrrhine primates. *Proc. Biol. Sci.* **279**, 715–721 (2012).
112. L. P. C. dos Santos, "Parâmetros nutricionais da dieta de duas populações de macacos-prego: *Sapajus libidinosus* no ecótono Cerrado/Caatinga e *Sapajus nigritus* na Mata Atlântica," PhD thesis, Universidade de São Paulo, São Paulo, Brazil (2015).
113. J. A. Chapman *et al.*, Meraculous: *De novo* genome assembly with short paired-end reads. *PLoS One* **6**, e23501 (2011).
114. G. Marçais, C. Kingsford, A fast, lock-free approach for efficient parallel counting of occurrences of *k*-mers. *Bioinformatics* **27**, 764–770 (2011).
115. B. Chevreux *et al.*, Using the miraEST assembler for reliable and automated mRNA transcript assembly and SNP detection in sequenced ESTs. *Genome Res.* **14**, 1147–1159 (2004).
116. C. Hahn, L. Bachmann, B. Chevreux, Reconstructing mitochondrial genomes directly from genomic next-generation sequencing reads—A baiting and iterative mapping approach. *Nucleic Acids Res.* **41**, e129 (2013).
117. A. F. A. Smit, R. Hubble, P. Green, RepeatMasker Open-4.0 2013-2015. www.repeatmasker.org.
118. A. F. A. Smit, R. Hubble, RepeatModeler Open-1.0 2008-2015. www.repeatmasker.org.
119. M. Stanke *et al.*, AUGUSTUS: Ab initio prediction of alternative transcripts. *Nucleic Acids Res.* **34**, W435–9 (2006).
120. S. Götz *et al.*, High-throughput functional annotation and data mining with the Blast2GO suite. *Nucleic Acids Res.* **36**, 3420–3435 (2008).
121. L. Li, C. J. Stoeckert Jr., D. S. Roos, OrthoMCL: Identification of ortholog groups for eukaryotic genomes. *Genome Res.* **13**, 2178–2189 (2003).
122. K. Katoh, D. M. Standley, MAFFT multiple sequence alignment software version 7: Improvements in performance and usability. *Mol. Biol. Evol.* **30**, 772–780 (2013).
123. Y. Benjamini, Y. Hochberg, Controlling the false discovery rate: A practical and powerful approach to multiple testing. *J. R. Stat. Soc. B* **57**, 289–300 (1995).
124. H. Byrne, Sape_Mango_1.1. NCBI Assembly. https://www.ncbi.nlm.nih.gov/assembly/GCA_022120495.1/#/def. Deposited 10 February.
125. H. Byrne, T. H. Webster, S. F. Brosnan, P. Izar, J. W. Lynch, Mango genome sequencing and assembly. NCBI. <https://www.ncbi.nlm.nih.gov/bioproject/?term=PRJNA717806>. Deposited 27 March 2021.
126. H. Byrne, T. H. Webster, S. F. Brosnan, P. Izar, J. W. Lynch, Mango mitochondrial genome. Zenodo. <https://zenodo.org/record/5225106#yudmxmByUl>. Deposited 19 August 2021.